

Rotating saddle trap as Foucault's pendulum.

O.N. Kirillov ¹, M. Levi ²

1 Helmholtz-Zentrum Dresden-Rossendorf, P.O. Box 510119, D-01314 Dresden, Germany

2 Department of Mathematics, Pennsylvania State University, University Park, PA 16802, USA.

Abstract

One of the few phenomena in mechanics that defy intuition is the stabilization of a particle in a rapidly rotating planar saddle potential. Besides the counterintuitive stabilization, an unexpected precessional motion is observed. In this note we show that this precession is due to a Coriolis-like force caused by the rotation of the potential. To our knowledge this is the first example where such force arises in an inertial reference frame.

Introduction

According to Earnshaw's theorem an electrostatic potential cannot have stable equilibria, i.e. the minima, since such potentials are harmonic functions. The theorem does not apply, however, if the potential depends on time; in fact, the 1989 Nobel Prize in physics was awarded to W. Paul [1] for his invention of the trap for suspending charged particles in an oscillating electric field. Paul's idea was to stabilize the saddle by "vibrating" the electrostatic field, by analogy with the so-called Stephenson-Kapitsa pendulum [2, 3, 4, 5, 6] in which the upside-down equilibrium is stabilized by vibration of the pivot. Instead of vibration, the saddle can also be stabilized by rotation of the potential (in two dimensions); this has been known for nearly a century: as early as 1918, L.E.J. Brouwer (1881–1966), one of the authors of the fixed point theorem in topology, considered stability of a heavy particle on a rotating slippery surface, [7, 8], Figure 1. The rotation-stabilized particles exhibit precession in the laboratory frame as illustrated in Figure 2. Up to now this precession has been explained by analyzing explicit solutions ([9, 10, 11]), leaving the underlying cause of this precession somewhat mysterious.

The non-dimensional equations of a particle in a rotating saddle potential can be written in the non-rotating (x, y, z) -frame, after a proper rescaling, as [11, 12]

$$\begin{aligned}\ddot{x} + x \cos 2\omega t + y \sin 2\omega t &= 0, \\ \ddot{y} + x \sin 2\omega t - y \cos 2\omega t &= 0,\end{aligned}\tag{1}$$

or in vector form

$$\ddot{\mathbf{x}} + S(\omega t)\mathbf{x} = \mathbf{0},\tag{2}$$

where

$$S(\omega t) = \begin{pmatrix} \cos 2\omega t & \sin 2\omega t \\ \sin 2\omega t & -\cos 2\omega t \end{pmatrix}, \quad \mathbf{x} = \begin{pmatrix} x \\ y \end{pmatrix}.\tag{3}$$

These equations are derived in the Appendix. For a heavy particle on a rotating saddle of Figure 1, the non-dimensional angular velocity is $\omega = \Omega/\sqrt{\kappa}$, where $\kappa = g/r$; the non-dimensional time t and dimensional time \hat{t} are related as $t = \hat{t}\Omega/\omega$ [7, 8].

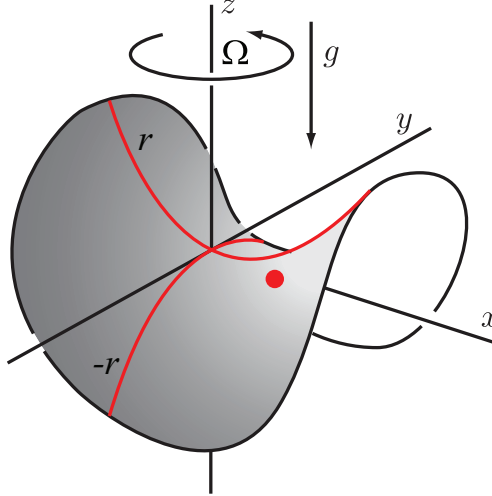


Figure 1: A unit mass on a saddle with the radii of the principal curvatures r and $-r$ that rotates with the angular velocity Ω in the gravitational field with acceleration g .

A geometrical interpretation of S . Note that $S(\tau)$ is a composition of the reflection with respect to the x -axis and the counterclockwise rotation through angle 2τ , Figure 3(A).

A “spinning arrows” interpretation of rotating saddle. As illustrated in Figure 3(B), the force field $-S(\omega t)\mathbf{x}$ of a rotating potential can be thought of in an entirely different way: starting with stationary saddle vector field $\langle x, -y \rangle$, we rotate each arrow of this field with angular velocity 2ω counterclockwise; the result is the same vector field $-\nabla U(\mathbf{x}, t)$.

Applications, connections to other systems.

Before getting to the point of this note, we mention that equations (1) arise in numerous applications across many seemingly unrelated branches of classical and modern physics [10, 12, 13, 14]; here is a partial list. They describe stability of a mass mounted on a non-circular weightless rotating shaft subject to a constant axial compression force [15, 16], in plasma physics they appear in the modeling of a stellatron – a high-current betatron with stellarator fields used for accelerating electron beams in helical quadrupole magnetic fields [9, 12, 17]. In quantum optics, equations (1) originate in the theory of rotating radio-frequency ion traps [11]. In celestial mechanics the rotating saddle equations describe linear stability of the triangular Lagrange libration points L_4 and L_5 in the restricted circular three-body problem [18, 19, 20]. In atomic physics the stable Lagrange points were produced in the Schrödinger-Lorentz atomic electron problem by applying a circularly polarized microwave field rotating in synchrony with an electron wave packet in a Rydberg atom [20]. This has led to a first observation of a non-dispersing Bohr wave packet localized near the Lagrange point while circling the atomic nucleus indefinitely [21]. Recently, the rotating saddle equations (1) reappeared in the study of confinement of massless Dirac particles, e.g. electrons in graphene [22]. Interestingly, stability of a rotating flow of a perfectly conducting ideal fluid in an

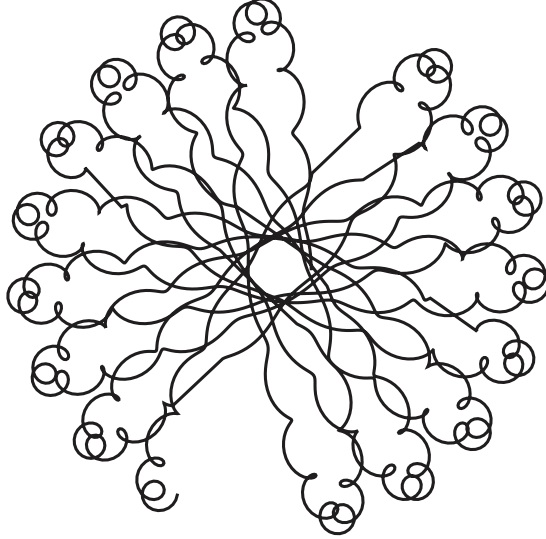


Figure 2: Prograde precession of a particle on a rotating saddle in the non-rotating frame for large angular velocity ω . In this illustration $\omega = 20/9 \approx 2.2$ (not even that large!).

azimuthal magnetic field possesses a mechanical analogy with the stability of Lagrange triangular equilibria and, consequently, with the gyroscopic stabilization on a rotating saddle [23]. As a final example in this list, (1) arise as linearized equations for a particle constrained to a saddle surface in gravitational field and rotating around the vertical axis, in the case when the two principal curvatures of the saddle are equal and opposite, Figure 1. The motion is stabilized [14, 16] for all sufficiently high ω . An illustration of a similar (but not equivalent) counterintuitive effect consists of a ball placed on a saddle surface rotating around the vertical axis and being in stable equilibrium at the saddle point [10]. We note however that the rolling ball on a surface is a non-holonomic system, entirely different from a particle sliding on a surface [24].

The result: a “hodograph” transformation.

The main point of this note is to show that the rapid rotation of the saddle gives rise to an unexpected Coriolis-like or magnetic-like force *in the laboratory frame*; it is this force that is responsible for prograde precession. To our knowledge this is the first example where the Coriolis-like force arises in the inertial frame.

To state the result we assign, to any motion $\mathbf{x} = \mathbf{x}(t)$ satisfying (2), its “guiding center”

$$\mathbf{u} = \mathbf{x} - \frac{\varepsilon^2}{4} S(\omega t)(\mathbf{x} - \varepsilon J \dot{\mathbf{x}}), \quad (4)$$

where $\varepsilon = \omega^{-1}$ and where J is the counterclockwise rotation by $\pi/2$:

$$J = \begin{pmatrix} 0 & -1 \\ 1 & 0 \end{pmatrix}.$$

We discovered that for large ω , i.e. small ε , the guiding center has a very simple dynamics:

$$\ddot{\mathbf{u}} - \frac{\varepsilon^3}{4} J \dot{\mathbf{u}} + \frac{\varepsilon^2}{4} \mathbf{u} = O(\varepsilon^4); \quad (5)$$

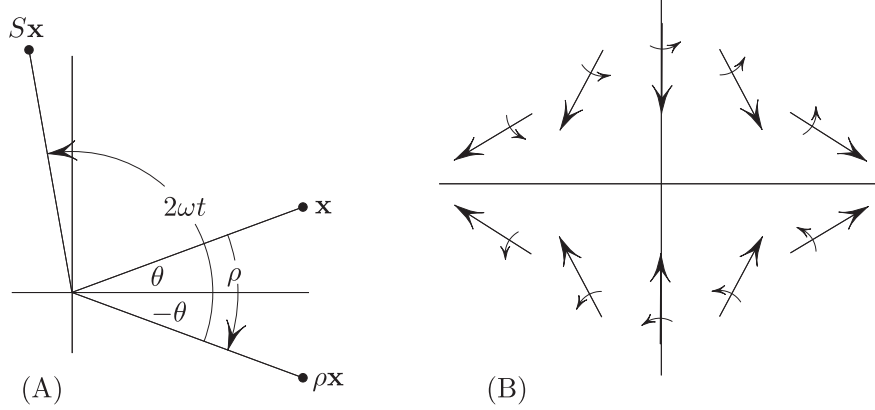


Figure 3: (A): S is a reflection followed by a rotation. (B). Another interpretation of the rotating saddle: rotating the potential with angular velocity ω amounts to rotating each arrow of the vector field $\langle x, -y \rangle$ with angular velocity 2ω .

that is, ignoring the ε^4 -terms, \mathbf{u} behaves as a particle with a Hookean restoring force $-\frac{\varepsilon^2}{4}\mathbf{u}$ and subject to the Coriolis- or magnetic- like force $\frac{\varepsilon^3}{4}J\dot{\mathbf{u}}$. Figure 4 shows a typical trajectory of the truncated equation

$$\ddot{\mathbf{u}} - \frac{\varepsilon^3}{4}J\dot{\mathbf{u}} + \frac{\varepsilon^2}{4}\mathbf{u} = 0. \quad (6)$$

This is in fact the motion of a Foucault pendulum, and just as in the Foucault pendulum [25] the Coriolis-like term is responsible for prograde precession of \mathbf{u} and thus of its “follower” \mathbf{x} .

Angular velocity of precession in (6) compared to earlier results. Angular velocity of precession of solutions of the Foucault-type equation (6) turns out to be $\Omega_p = \varepsilon^3/8$. Indeed, writing the equation in the frame rotating with angular velocity Ω_p gives rise to a Coriolis term and a centrifugal term, and the system in that frame becomes

$$\ddot{\mathbf{z}} + 2\Omega_p J\dot{\mathbf{z}} - \frac{\varepsilon^3}{4}J\dot{\mathbf{z}} + \frac{\varepsilon^2}{4}\mathbf{z} + \Omega_p^2\mathbf{z} = 0.$$

With the alleged value of Ω_p , the second and the third terms cancel, and the resulting system

$$\ddot{\mathbf{z}} + (\varepsilon^2/4 + \varepsilon^6/64)\mathbf{z} = 0$$

exhibits no precession (all solutions are simply ellipses). We conclude that $\varepsilon^3/8$ is indeed the angular velocity of precession of \mathbf{u} .

For the heavy particle on a rotating saddle of Figure 1 we express the frequency of precession in the dimensional form using the scaling transformations. Indeed,

$$\frac{\varepsilon^3}{8}t = \frac{\varepsilon^3}{8}\varepsilon\Omega\hat{t} = \frac{\kappa^2}{8\Omega^3}\hat{t}.$$

The dimensional precession frequency of the particle in Figure 1 is thus $\frac{\kappa^2}{8\Omega^3}$. Assuming, for instance, $\kappa = 2q$ and $\Omega = 1$, yields the expression $q^2/2$ for the precession frequency

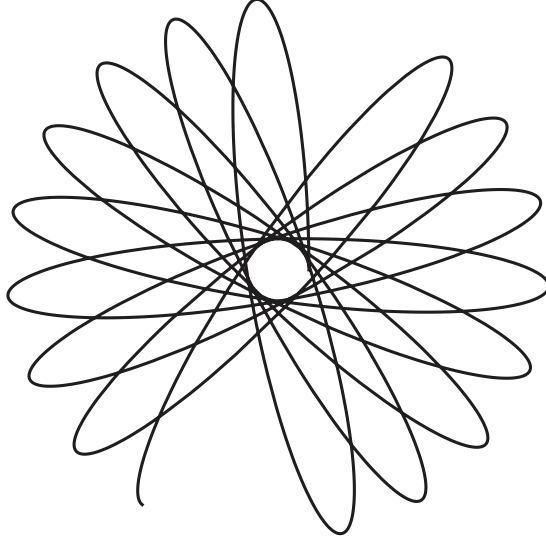


Figure 4: The motion of the “guiding center”, governed by (5), is the same as that of a Foucault pendulum. Here $\varepsilon = 0.45$.

that was found in the work [11]. Similarly, the dimensional analog of the frequency $\varepsilon/2$ of the secular oscillations is $\frac{|\kappa|}{2\Omega}$, which follows from the relations:

$$\frac{\varepsilon}{2}t = \frac{\varepsilon}{2}\varepsilon\Omega\hat{t} = \frac{|\kappa|}{2\Omega}\hat{t}.$$

Again, at $\kappa = 2q$ and $\Omega = 1$ we reproduce the secular frequency q of the work [11].

A Coriolis-like force in the inertial frame. If $\frac{\varepsilon^3}{4}J\dot{\mathbf{u}}$ were a true Coriolis force, it would have been due to the rotation of the reference frame with angular velocity $\frac{\varepsilon^3}{8}$ – but our frame is inertial. Alternatively, one can think of $\frac{\varepsilon^3}{4}J\dot{\mathbf{u}}$ as the Lorentz force exerted on a charge (of unit mass and of unit charge) in constant magnetic field $B = \frac{\varepsilon^3}{4}$ perpendicular to the plane. Rapid rotation of the saddle gives rise to a virtual pseudo-magnetic force (cf. [26, 27, 28]); as one implication, the asteroids in the vicinity of Lagrange triangular equilibria behave like charged particles in a weak magnetic field, from the inertial observer’s point of view.

A numerical illustration. Figure 5 shows a solution \mathbf{x} alongside its “guiding center” \mathbf{u} . We note, as a side remark, that near the origin the solution follows the trajectory of the guiding center rather closely, reflecting the fact that oscillatory micromotion is small near the origin, as is clear from the governing equations (1).

We discovered the transformation (4) via a somewhat lengthy normal form argument [5, 6] which, due to its length, will be presented elsewhere. Nevertheless, once the transformation (4) has been produced, the statement (5) can be verified directly by substituting (4) into (2); we omit the routine but slightly lengthy details, but give a geometrical view of this transformation.

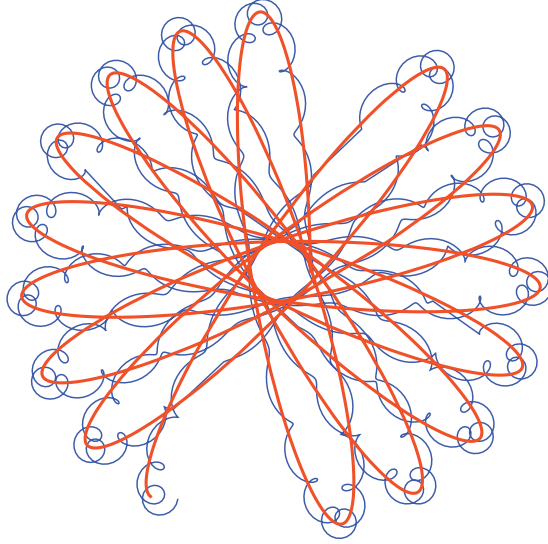


Figure 5: A trajectory of the guiding center \mathbf{u} (in red) tracking the corresponding trajectory \mathbf{x} . The view is in the inertial frame. $\varepsilon = 0.45$.

A geometrical view of the hodograph transformation. Our result says, in effect, that the “jiggle” term

$$\frac{\varepsilon^2}{4}S(\omega t)(\mathbf{x} - \varepsilon J\dot{\mathbf{x}})$$

in (4), when subtracted from \mathbf{x} , leaves a smooth motion.¹ Figure 6 gives a geometrical view of this term. It is still an open problem to find a simple heuristic explanation of choice of the term $-\varepsilon J\dot{\mathbf{x}}$ in (4). Finding a heuristic explanation of the “magnetic” term $\frac{\varepsilon^3}{4}J\dot{\mathbf{u}}$ remains an open problem as well.

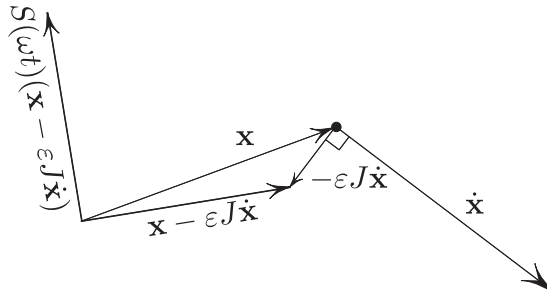


Figure 6: A geometrical representation of the “jiggle” term $S(\omega t)(\mathbf{x} - \varepsilon J\dot{\mathbf{x}})$ (without the $\varepsilon^2/4$ factor) in the hodograph transformation. A geometrical interpretation of S is shown in Figure 3(A).

Validity of the truncation. Our result says that the fictitious particle \mathbf{u} , which shadows the solution \mathbf{x} , is subject to two forces $-(\varepsilon^3/4)\dot{\mathbf{u}} - (\varepsilon^2/4)\mathbf{u}$, plus a smaller $O(\varepsilon^4)$ -force.

What is the cumulative effect of this force? One can show, using standard results of perturbation theory, that neglecting the $O(\varepsilon^4)$ -term causes the deviation less than $c_1\varepsilon^3$

¹as far as the powers up to ε^3 are concerned.

over the time $|t| < c_2 \varepsilon^{-2}$ for some constants c_1, c_2 , for all ε sufficiently small. As it often happens with rigorous results, this one is overly pessimistic: computer simulations show that “sufficiently small” is actually not that small: for example, $\varepsilon = 0.45$ in Figure 5. In fact, the reason for such an unexpectedly good agreement is the fact that the error on the right-hand side is actually $O(\varepsilon^6)$ – two orders better than claimed, as follows from an explicit computation by Michael Berry, [29]. We do not focus on the analysis of higher powers of ε because it would only add *higher-order* corrections to the coefficients on the left-hand side of (5), without affecting our main point (namely, that an unexpected Coriolis-like force appears).²

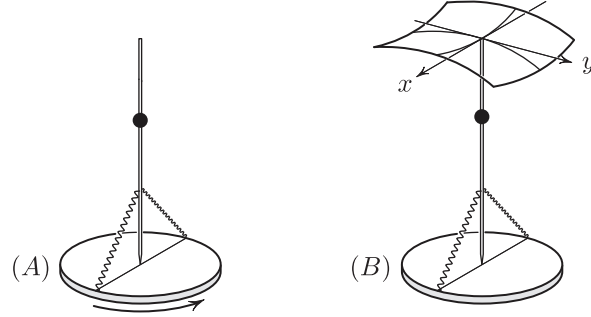


Figure 7: A mechanical realization of the rotating saddle trap. Here x, y are the angular variables, and the graph of the potential energy in terms of the angular variables x, y is shown.

An experiment.

Figure 7 illustrates a mechanical implementation of the rotating saddle trap (cf. [15, 16]). As we had mentioned in the introduction, a ball rolling on the rotating saddle surface [10] is *not* the right physical realization of the rotating saddle trap because (i) the friction is very hard to eliminate, and, perhaps more importantly, because the rolling ball does not behave as a sliding particle. In fact, the rolling ball can be stable even *on top* of a sphere rotating around its vertical diameter [30]!

A light rod with a massive ball in Figure 7 is essentially an inverted spherical pendulum; the sharpened end of the rod, resting on the center of the platform, acts as a ball joint with the horizontal plane. The height of the ball is adjustable, like in a *metronome*. If the ball is placed sufficiently low then the two springs will stabilize the pendulum in the x -direction, Figure 7(B),³ and the potential acquires a saddle shape

²According to M. Berry’s computation [29] based on explicit solution of (1), replacing the coefficient $\varepsilon^2/4$ in (6) by

$$\frac{\varepsilon^2}{4} \left(1 + \frac{3}{16} \varepsilon^4 + \frac{11}{128} \varepsilon^8 + \dots \right) = -\frac{(1 - \sqrt{1 - \varepsilon^2})(1 - \sqrt{1 + \varepsilon^2})}{\varepsilon^2},$$

and replacing the coefficient $\varepsilon^3/4$ by

$$\frac{\varepsilon^3}{4} \left(1 + \frac{5}{16} \varepsilon^4 + \frac{21}{128} \varepsilon^8 + \dots \right) = \frac{2}{\varepsilon} - \frac{\sqrt{1 - \varepsilon^2} + \sqrt{1 + \varepsilon^2}}{\varepsilon}.$$

yields the equation for the exact guiding center (the expression for which is then given by (4) which includes higher order terms).

³here x and y are angular variables.

(since the y -direction is unstable):

$$U_0(x, y) = \frac{1}{2} (ax^2 - by^2),$$

with $a, b > 0$, ignoring higher powers of x, y . Here $b = g/L$, where L is the distance from the ball to the sharpened end of the rod. In the next paragraph we suggest a simple way to adjust L to make the two curvatures equal: $a = b$, so that the linearized equations become

$$\ddot{\mathbf{x}} + bS(\Omega t)\mathbf{x} = 0, \quad b = \frac{g}{L}$$

a rescaled version of (1). By rescaling the physical time t to the non-dimensional time $\tau = \sqrt{at}$, and introducing

$$\omega = \Omega/\sqrt{a}, \tag{7}$$

we transform the above equation into the non-dimensional form (1) (after renaming τ back to t), which is stable if $\omega > 1$ [7, 14, 16]. Now $a = b = g/L$, where L is the distance from the mass to the ball joint, and (7) gives us the length

$$L = g \left(\frac{\omega}{\Omega} \right)^2. \tag{8}$$

The 78 rpm of a vinyl record player corresponds to $\Omega \approx 8.2 \text{sec}^{-1}$, and the value $\omega \approx 2.2$ referred to in Figure 2 corresponds to the height $L \approx 71 \text{cm}$. How short can we make the pendulum without losing stability? The cutoff length is $L \approx 14 \text{cm}$, as follows from (8) and the fact that (1) is stable if and only if $\omega > 1$. Incidentally, large L corresponds to large ω , according to (8) (for fixed rpm). This makes intuitive sense, since a “natural” unit of time in our system is the period $2\pi\sqrt{L/g}$ of the oscillations along the stable axis of the stationary potential; for large L this period is long, and during it the rotating potential will spin many times, corresponding to large ω .

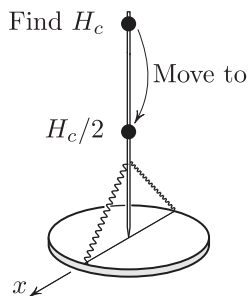


Figure 8: How to find the length for which the curvatures of the saddle are equal and opposite: $U_{xx}(0,0) = -U_{yy}(0,0)$: find by trial and error the height H_c at which the x -direction changes stability, and half H_c .

How to (easily) realize the saddle with equal principal curvatures. It may seem (as it did to us initially) that one needs to measure the stiffnesses of the springs, the various lengths in Figure 7, the mass of the ball, and then use these to compute the value of L . Instead, here is a way to avoid all this work. Referring to Figure 8, *adjust the position of the massive ball along the rod to such critical height H_c as to make the*

ball neutrally stable in the x -direction: if the ball is too high, it will be unstable in the x -direction; if the ball is too low, it will be stable in the x -direction; a bisection method will quickly lead to a good approximation to H_c . Remarkably, the desired “equal curvatures” height of the ball is simply

$$L = \frac{H_c}{2}.$$

An explanation. The angle y satisfies the inverted pendulum equation $\ddot{y} - \frac{g}{L} \sin y = 0$, which for small angles is well approximated by

$$\ddot{y} - \frac{g}{L}y = 0.$$

Similarly, the linearized equation for the angle x is

$$\ddot{x} + \left(-\frac{g}{L} + \frac{k}{L^2} \right) x = 0;$$

L is not yet chosen and k depends on the parameters of the system, but not on L .⁴ Our goal is to find L such that the coefficients in the above equations are equal and opposite, which amounts to asking for L satisfying $\frac{g}{L} = -\frac{g}{L} + \frac{k}{L^2}$, or

$$2Lg = k. \tag{9}$$

We now relate the unknown k to H_c . For the pendulum of the length H_c the angle x satisfies $\ddot{x} + \left(-\frac{g}{H_c} + \frac{k}{H_c^2} \right) x = 0$, with the coefficient $-\frac{g}{H_c} + \frac{k}{H_c^2} = 0$ since the equilibrium is neutral; this gives

$$k = gH_c.$$

Substituting $H_c = 2L$ into the last equation gives (9) – precisely the condition for the equality of the coefficients in U .

Conclusion. We showed that the rapid rotation of the saddle potential creates a weak Lorentz-like, or a Coriolis-like force, in addition to an effective stabilizing potential – all in the inertial frame. We also proposed a simple experiment to demonstrate the phenomenon.

Appendix: Deriving the equations of motion.

The motion of a point unit mass $\mathbf{x} = (x, y)$ in any time-dependent potential $U(x, y, t)$ is given by

$$\ddot{\mathbf{x}} = -\nabla U(\mathbf{x}, t) \tag{10}$$

(the gradient here is taken with respect to the (x, y) -coordinates). The graph of our $U(\mathbf{x}, t)$ is obtained by rotating the graph of $U_0(x, y) = \frac{1}{2}(x^2 - y^2)$, and must (i) find the expression for this rotated potential $U(\mathbf{x}, t)$, and (ii) compute ∇U – hopefully in an elegant way, without brute force.

⁴Specifically, k depends on the springs’ stiffness, on the angle they form with the diameter in Figure 7 and on the ball’s mass (to which it is inversely proportional). But an easier way to find k is to note that $k = gH_c$, as we show below.

The answer to (i) is simply

$$U(\mathbf{x}, t) = U_0(R^{-1}\mathbf{x}), \quad (11)$$

where $R = R(\omega t)$ denotes the rotation through the angle ωt around the origin (counterclockwise if $t > 0$) and is given by the matrix

$$R = R(\omega t) = \begin{pmatrix} \cos \omega t & -\sin \omega t \\ \sin \omega t & \cos \omega t \end{pmatrix}; \quad (12)$$

Figure 9 explains why: Imagine looking down upon the graph of $U(\mathbf{x}, t)$, Figure 9(A),

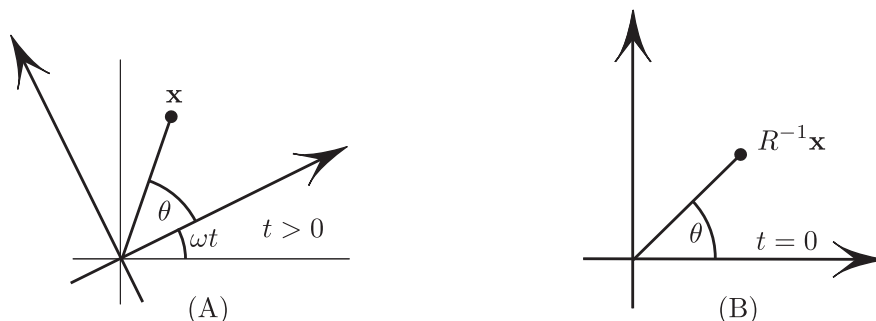


Figure 9: Explanation of (11).

focusing on a point \mathbf{x} ; let us now rotate the graph *together with* the point \mathbf{x} clockwise by angle ωt , thereby turning the graph into the graph of U_0 ; the result is shown in (B). Since the graph and the point \mathbf{x} rotated together, the height above \mathbf{x} remained unchanged – exactly what (11) says!

(ii) to find ∇U we could write (11) in terms of x and y and then differentiate, but here is a more elegant mess-avoiding way: let us write $U_0(\mathbf{x}) = \frac{1}{2}(x^2 - y^2)$ as the dot product:

$$U_0(\mathbf{x}) = \frac{1}{2}\langle \rho \mathbf{x}, \mathbf{x} \rangle, \quad \text{where } \rho = \text{diag}(1, -1)$$

(note that ρ is the mirror reflection in the y -axis), and use this in (11):

$$U(\mathbf{x}, t) = \frac{1}{2}\langle \rho R^{-1}\mathbf{x}, R^{-1}\mathbf{x} \rangle = \frac{1}{2}\langle R\rho R^{-1}\mathbf{x}, \mathbf{x} \rangle = \frac{1}{2}\langle S\mathbf{x}, \mathbf{x} \rangle; \quad (13)$$

in (13) we used the fact that R is an orthogonal matrix. Multiplying out $R\rho R^{-1} = S$ gives the matrix S defined by equation (3).

Now for any symmetric matrix S , one has $\nabla\langle S\mathbf{x}, \mathbf{x} \rangle = 2S\mathbf{x}$, as one can see with almost no computation⁵, and we conclude

$$\nabla U(\mathbf{x}, t) = S\mathbf{x};$$

Equation of motion (10) turns into (2), as claimed.

Acknowledgement Mark Levi gratefully acknowledges support by the NSF grant DMS-0605878.

⁵Indeed, the definition of the gradient of a function f states: $\langle \nabla f(\mathbf{x}), \mathbf{v} \rangle \stackrel{\text{def}}{=} \frac{d}{ds} f(\mathbf{x} + s\mathbf{v})_{s=0}$ for all vectors \mathbf{v} . In our case, $f(\mathbf{x}) = \langle S\mathbf{x}, \mathbf{x} \rangle$ and $\frac{d}{ds} f(\mathbf{x} + s\mathbf{v})_{s=0} = \langle 2S\mathbf{x}, \mathbf{v} \rangle$; comparing this with the left-hand side of the definition proves $\nabla\langle S\mathbf{x}, \mathbf{x} \rangle = 2S\mathbf{x}$.

References

- [1] W. Paul, Electromagnetic traps for charged and neutral particles, *Rev. Mod. Phys.*, 62, 531–540, 1990.
- [2] A. Stephenson, On an induced stability, *Phil. Mag.*, 15, 233, 1908.
- [3] P. L. Kapitsa, Pendulum with a vibrating suspension, *Usp. Fiz. Nauk*, 44, 7–15, 1951.
- [4] L. D. Landau, E. M. Lifshitz (1960). *Mechanics. Vol. 1 (1st ed.)*. Pergamon Press.
- [5] M. Levi, Geometry of Kapitsa’s potentials, *Nonlinearity*, 11, 1365–1368, 1998.
- [6] M. Levi, Geometry and physics of averaging with applications, *Physica D*, 132, 150–164, 1999.
- [7] L. E. J. Brouwer, Beweging van een materieel punt op den bodem eener draaiende vaas onder den invloed der zwaartekracht, *N. Arch. v. Wisk.*, 2, 407–419, 1918.
- [8] O. Bottema, Stability of equilibrium of a heavy particle on a rotating surface, *ZAMP Z. angew. Math. Phys.*, 27, 663–669, 1976.
- [9] R. M. Pearce, Strong focussing in a magnetic helical quadrupole channel, *Nuclear instruments and methods*, 83(1), 101–108, 1970.
- [10] R. I. Thompson, T. J. Harmon, M. G. Ball, The rotating-saddle trap: a mechanical analogy to RF-electric-quadrupole ion trapping? *Canadian Journal of Physics*, 80, 1433–1448, 2002.
- [11] T. Hasegawa, J. J. Bollinger, Rotating-radio-frequency ion traps, *Phys. Rev. A*, 72, 043403, 2005.
- [12] V. E. Shapiro, Rotating class of parametric resonance processes in coupled oscillators, *Phys. Lett. A*, 290, 288–296, 2001.
- [13] O. N. Kirillov, Exceptional and diabolical points in stability questions. *Fortschritte der Physik - Progress in Physics*, 61(2-3), 205–224, 2013.
- [14] O. N. Kirillov, *Nonconservative Stability Problems of Modern Physics*, (2013) De Gruyter, Berlin, Boston, 429p.
- [15] D. J. Inman, A sufficient condition for the stability of conservative gyroscopic systems, *Trans. ASME J. Appl. Mech.*, 55, 895–898, 1988.
- [16] K. Veselic, On the stability of rotating systems, *ZAMM Z. angew. Math. Mech.*, 75, 325–328, 1995.
- [17] C. W. Roberson, A. Mondelli, D. Chernin, High-current betatron with stellarator fields, *Phys. Rev. Lett.*, 50, 507–510, 1983.
- [18] M. Gascheau, Examen d’une classe d’équations différentielles et application à un cas particulier du probleme des trois corps, *Comptes Rendus*, 16, 393–394, 1843.

- [19] K. T. Alfriend, The stability of the triangular Lagrangian points for commensurability of order two, *Celestial Mechanics*, 1(3–4), 351–359, 1970.
- [20] I. Bialynicki-Birula, M. Kaliński, J. H. Eberly, Lagrange equilibrium points in celestial mechanics and nonspreading wave packets for strongly driven Rydberg electrons, *Phys. Rev. Lett.*, 73, 1777–1780, 1994.
- [21] H. Maeda, J. H. Gurian, T. F. Gallagher, Nondispersing Bohr wave packets, *Phys. Rev. Lett.*, 102, 103001, 2009.
- [22] J. Nilsson, Trapping massless Dirac particles in a rotating saddle, *Phys. Rev. Lett.*, 111, 100403, 2013.
- [23] G. I. Ogilvie, J. E. Pringle, The non-axisymmetric instability of a cylindrical shear flow containing an azimuthal magnetic field, *Mon. Not. R. Astron. Soc.*, 279, 152–164, 1996.
- [24] Ju. I. Neimark, N. A. Fufaev, *Dynamics of Nonholonomic Systems (Translations of Mathematical Monographs, V. 33)*, American Mathematical Society, Providence, RI, 2004.
- [25] A. Khein, D. F. Nelson, Hannay angle study of the Foucault pendulum in action-angle variables, *Am. J. Phys.* 61(2), 170–174, 1993.
- [26] M. V. Berry, J. M. Robbins, Chaotic classical and half-classical adiabatic reactions: geometric magnetism and deterministic friction, *Proc. R. Soc. A* 442, 659–672, 1993.
- [27] M. V. Berry, P. Shukla, High-order classical adiabatic reaction forces: slow manifold for a spin model, *J. Phys. A: Math. Theor.* 43, 045102, 2010.
- [28] M. V. Berry, P. Shukla, Slow manifold and Hannay angle for the spinning top, *Eur. J. Phys.* 32, 115–127, 2011.
- [29] M. V. Berry, Private communication, 15 February, 2015.
- [30] W. Weckesser, A ball rolling on a freely spinning turntable, *Am. J. Phys.*, 65, 736–738, 1997.